

Husimi distribution and phase-space analysis of a vibron-model quantum phase transition

M. Calixto

Departamento de Matemática Aplicada, Universidad de Granada, Fuentenueva s/n, 18071 Granada, Spain

R. del Real

*Departamento de Física Atómica, Molecular y Nuclear,
Universidad de Granada, Fuentenueva s/n, 18071 Granada, Spain*

E. Romera

*Departamento de Física Atómica, Molecular y Nuclear and Instituto Carlos I de Física Teórica y Computacional,
Universidad de Granada, Fuentenueva s/n, 18071 Granada, Spain*

(Dated: September 22, 2014)

The Husimi distribution is proposed for a phase space analysis of quantum phase transitions in the two-dimensional $U(3)$ vibron model for N -size molecules. We show that the inverse participation ratio and Wehrl's entropy of the Husimi distribution give sharp signatures of the quantum (shape) phase transition from linear to bent. Numerical results are complemented with a variational approach using parity-symmetry-adapted $U(3)$ coherent states, which reach the minimum Wehrl entropy $\frac{N(3+2N)}{(N+1)(N+2)}$, in the rigidly linear phase, according to a generalized Wehrl-Lieb conjecture. We also propose a characterization of the vibron-model quantum phase transition by means of the zeros of the Husimi distribution.

I. INTRODUCTION

Quantum Phase Transitions (QPTs) have become an important subject in quantum many body problems [1]. Unlike classical phase transitions, QPTs take place at absolute zero of temperature. Generally speaking, one finds different quantum phases connected to specific geometric configurations of the ground state and related to distinct dynamic symmetries of the Hamiltonian. The QPT occurs as a function of a control parameter ξ that appears in the Hamiltonian H . For us it will appear in the form of a convex combination $H(\xi) = (1 - \xi)H_1 + \xi H_2$. At $\xi = 0$ the system is in phase I, characterized by the dynamical symmetry G_1 of H_1 , and at $\xi = 1$ the system is in phase II, characterized by the dynamical symmetry G_2 of H_2 . At some critical point $\xi_c \in (0, 1)$ there is an abrupt change in the symmetry and structure of the ground state wavefunction. This is the case of the so-called 'vibron models' (see e.g. [2–5]), interacting boson models which exhibits a second order shape phase transition from linear to bent. These models have been used to study the rovibrational properties in diatomic and polyatomic molecules and have turned to be very useful to study symmetry properties of quantum systems. Other interesting model exhibiting a QPT is the case of an ensemble of atoms interacting with a single bosonic field mode described by the Dicke Hamiltonian [6], which shares some features with the present vibron model.

In Quantum Mechanics we have to our disposal several distributions to characterize phase-space properties [7]. On the one hand, the Wigner function, widely used in Quantum Optics. On the other hand, the Husimi distribution, which is given by the overlap between a minimal uncertainty (coherent) state and the wavefunction. This

distribution proves sometimes more convenient because, unlike Wigner distribution, it is non-negative. Husimi distribution has been found useful for a phase-space visualization of a metal-insulator transition [8], to analyze quantum chaos in atomic physics [9] or to analyze models in condensed matter physics [10]. In addition, we would like to point out that the zeros of the Husimi distribution have essential information, in particular, the quantum state can be described by its distribution of zeros [11]. They are the least probable points in phase space and they have also been considered as a quantum indicator of classical and quantum chaos [12, 13].

The Husimi distribution has a great amount of information and it can be useful to consider informational measures as the so-called inverse participation ratio and Wehrl entropy [14]. An analysis of the Dicke-model QPT by means of information measures has been done in position and momentum spaces, separately [15–18, 20] and through the Husimi distribution, its marginals and its participation ratio and Wehrl entropy [21]. Moreover, QPT has been characterized by means of the zeros of the Husimi distribution in the Dicke model [21]. Here we shall offer an informational description of the vibron-model QPT in phase space in terms of the inverse participation ratio (and higher moments) and the Wehrl entropy of the Husimi distribution. Additionally we shall investigate the visualization of the vibron-model QPT through the zeros of the Husimi distribution.

This article is organized as follows. In Section II we briefly remind the vibron-model Hamiltonian, introduce coherent states and the Husimi distribution of the ground state, and present the inverse participation ratio and the Wehrl entropy for the Husimi distribution in a numerical framework. In Section III we study a variational approximation to the ground state wave function in terms of

symmetry-adapted coherent states and analyze the information measures for this approximation in the thermodynamic limit. Zeros of the Husimi (ansatz) distribution are also computed in order to characterize the QPT.

II. VIBRON MODEL AND HUSIMI DISTRIBUTION

2D-vibron models describe a system containing a dipole degree of freedom constrained to planar motion. Elementary excitations are (creation and annihilation) 2D vector τ -bosons $\{\tau_x^\dagger, \tau_y^\dagger, \tau_x, \tau_y\}$ and a scalar σ -boson $\{\sigma^\dagger, \sigma\}$. It is convenient to introduce circular bosons: $\tau_\pm = \mp(\tau_x \mp i\tau_y)/\sqrt{2}$. The nine generators of the $U(3)$ algebra are bilinear products of creation and annihilation operators, in particular:

$$\begin{aligned}\hat{n} &= \tau_+^\dagger \tau_+ + \tau_-^\dagger \tau_-, \quad \hat{n}_s = \sigma^\dagger \sigma, \\ \hat{l} &= \tau_+^\dagger \tau_+ - \tau_-^\dagger \tau_-, \\ \hat{D}_+ &= \sqrt{2}(\tau_+^\dagger \sigma - \sigma^\dagger \tau_-), \quad \hat{D}_- = \sqrt{2}(-\tau_-^\dagger \sigma + \sigma^\dagger \tau_+),\end{aligned}\quad (1)$$

denote the number operator of vector \hat{n} and scalar \hat{n}_s bosons, 2D angular momentum \hat{l} and dipole \hat{D}_\pm operators, respectively (see [5] for the reminder four operators \hat{Q}_\pm, \hat{R}_\pm , which will not be used here). Assuming the total number of bosons $\hat{N} = \hat{n} + \hat{n}_s$ and the 2D angular momentum \hat{l} to be conserved, there are only two dynamical symmetry limits, $G_1 = U(2)$ and $G_2 = SO(3)$, associated with two algebraic chains starting from $U(3)$ and ending in $SO(2)$: the so-called ‘cylindrical’ and ‘displaced’ oscillator chains. A general Hamiltonian of the $U(3)$ vibron model with only one- and two-body interactions can be expressed in terms of linear and quadratic Casimir operators of all the subalgebras contained in the dynamical symmetry algebra chains. To capture the essentials of the phase transition from the G_1 -phase (linear) to the G_2 -phase (bent) it is enough to consider a convex combination of the linear $C_1(U(2)) = \hat{n}$ and quadratic $C_2(SO(3)) = \hat{W}^2 = (\hat{D}_+ \hat{D}_- + \hat{D}_- \hat{D}_+)/2 + \hat{l}^2$ Casimir operators of the corresponding dynamical symmetries. In particular, we shall consider the essential Hamiltonian [5]

$$\hat{H} = (1 - \xi)\hat{n} + \xi \frac{N(N+1) - \hat{W}^2}{N-1}, \quad (2)$$

where the (constant) quantum number N is the total number of bound states that labels the totally symmetric $(N+1)(N+2)/2$ dimensional representation $[N]$ of $U(3)$. It is known (see [5] and later on Sec. III) that this model exhibits a (shape) QPT at $\xi_c = 0.2$ and we shall see that Wehrl entropies provide sharp indicators of this QPT.

The Hilbert space is spanned by the orthonormal basis vectors

$$|N; n, l\rangle = \frac{(\sigma^\dagger)^{N-n} (\tau_+^\dagger)^{\frac{n+l}{2}} (\tau_-^\dagger)^{\frac{n-l}{2}}}{\sqrt{(N-n)! \left(\frac{n+l}{2}\right)! \left(\frac{n-l}{2}\right)!}} |0\rangle, \quad (3)$$

where the bending quantum number $n = N, N-1, N-2, \dots, 0$ and the angular momentum $l = \pm n, \pm(n-2), \dots, \pm 1$ or 0 (n =odd or even) are the eigenvalues of \hat{n} and \hat{l} , respectively. The matrix elements of \hat{W}^2 can be easily derived (see e.g. [5]):

$$\begin{aligned}\langle N; n', l | \hat{W}^2 | N; n, l \rangle &= \\ &((N-n)(n+2) + (N-n+1)n + l^2)\delta_{n',n} \\ &- ((N-n+2)(N-n+1)(n+l)(n-l))^{\frac{1}{2}}\delta_{n',n-2} \\ &- ((N-n)(N-n-1)(n+l+2)(n-l+2))^{\frac{1}{2}}\delta_{n',n+2}.\end{aligned}$$

From these matrix elements, it is easy to see that time evolution preserves the parity $e^{i\pi n}$ of a given state $|N; n, l\rangle$. That is, the parity operator $\hat{\Pi} = e^{i\pi \hat{n}}$ commutes with \hat{H} and both operators can then be jointly diagonalized. We shall take this fact into account when proposing parity-symmetry-adapted ansatzes in subsection III.

A. $SU(3)$ coherent states and Husimi distribution

Let us use the notation $(a_0, a_1, a_2) \equiv (\sigma, \tau_+, \tau_-)$ for our three oscillator operators. $SU(3)$ projective coherent states (CSs) are defined as (for a given N)

$$\begin{aligned}|z_1, z_2\rangle &\equiv \frac{(a_0^\dagger + z_1 a_1^\dagger + z_2 a_2^\dagger)^N |0\rangle}{N!(1 + |z_1|^2 + |z_2|^2)^{N/2}} \\ &= \sum_{n=0}^N \sum_{m=0}^n \varphi_{n,m}^{(N)}(z_1, z_2) |N; n, l = n - 2m\rangle, \quad (4)\end{aligned}$$

with $z_1, z_2 \in \mathbb{C}$ and

$$\varphi_{n,m}^{(N)}(z_1, z_2) \equiv \frac{(N!/((N-n)!(n-m)!m!))^{1/2}}{(1 + |z_1|^2 + |z_2|^2)^{N/2}} z_1^{n-m} z_2^m. \quad (5)$$

They can be seen as a generalization of $SU(2)$ spin- j coherent states:

$$|z\rangle = (1 + |z|^2)^{-j} \sum_{m=-j}^j \binom{2j}{j+m}^{1/2} z^{j+m} |j, m\rangle, \quad (6)$$

in terms of angular momentum or Dicke states $|j, m\rangle$.

Although $SU(3)$ projective CSs are not an orthonormal set since

$$\langle z_1, z_2 | z'_1, z'_2 \rangle = \frac{(1 + \bar{z}_1 z'_1 + \bar{z}_2 z'_2)^N}{(1 + |z_1|^2 + |z_2|^2)^{N/2} (1 + |z'_1|^2 + |z'_2|^2)^{N/2}}, \quad (7)$$

they form an overcomplete set of the corresponding Hilbert space and fulfill the closure relation or resolution of the identity (see e.g. [22]):

$$1 = \int_{\mathbb{R}^4} |z_1, z_2\rangle \langle z_1, z_2| d\mu(z_1, z_2), \quad (8)$$

with

$$d\mu(z_1, z_2) = \frac{(N+1)(N+2)}{\pi^2} \frac{d^2 z_1 d^2 z_2}{(1 + |z_1|^2 + |z_2|^2)^3} \quad (9)$$

the measure on the complex projective (quotient) space $\mathbb{CP}^2 = U(3)/U(1)^3$ and $d^2z_{1,2} \equiv d\text{Re}(z_{1,2})d\text{Im}(z_{1,2})$ the usual Lebesgue measure on \mathbb{R}^2 or \mathbb{C} . In general, the exact ground state vector ψ will be given as an expansion

$$|\psi_\xi^{(N)}\rangle = \sum_{n=0}^N \sum_{m=0}^n c_{nm}^{(N)}(\xi) |N; n, l = n - 2m\rangle, \quad (10)$$

where the coefficients $c_{nm}^{(N)}(\xi)$ are calculated by numerical diagonalization of (2). One can realize that the ground state $|\psi_\xi^{(N)}\rangle$ has even-parity since, for instance, $c_{nm}^{(N)}(\xi) = 0$ for n odd.

The Husimi distribution $\Psi_\xi^{(N)}(z_1, z_2)$ of $\psi_\xi^{(N)}$ is, by definition, given by the squared modulus of the overlap between $|\psi_\xi^{(N)}\rangle$ and an arbitrary coherent state $|z_1, z_2\rangle$, that is:

$$\begin{aligned} \Psi_\xi^{(N)}(z_1, z_2) &= |\langle z_1, z_2 | \psi_\xi^{(N)} \rangle|^2 \\ &= \sum_{n,n'=0}^N \sum_{m,m'=0}^n c_{nm}^{(N)}(\xi) \bar{c}_{n'm'}^{(N)}(\xi) \\ &\quad \times \varphi_{n,m}^{(N)}(z_1, z_2) \varphi_{n',m'}^{(N)}(\bar{z}_1, \bar{z}_2) \end{aligned} \quad (11)$$

and normalized according to:

$$\int_{\mathbb{R}^4} \Psi_\xi^{(N)}(z_1, z_2) d\mu(z_1, z_2) = 1. \quad (12)$$

This can be seen as an alternative (coherent state) representation to the usual position q and momentum p representations traditionally given by $\psi(q) = \langle q | \psi \rangle$ and $\tilde{\psi}(p) = \langle p | \psi \rangle$, respectively (see [23] for the expression of $|\psi_\xi^{(N)}\rangle$ in position representation in terms of Hermite polynomials).

B. Moments and Rényi-Wehrl entropy of the Husimi distribution

Important quantities to visualize the QPT in the vibron model across the critical point ξ_c will be the ν -th moments of the Husimi distribution (11):

$$M_{N,\nu}(\xi) = \int_{\mathbb{R}^4} (\Psi_\xi^{(N)}(z_1, z_2))^\nu d\mu(z_1, z_2). \quad (13)$$

Note that $M_{N,1} = 1$ since $\Psi_\xi^{(N)}$ is normalized (12). Among all moments we shall single-out the so-called “inverse participation ratio” (IPR) $P_N(\xi) = M_{N,2}(\xi)$ which somehow measures the (de-)localization of $\Psi_\xi^{(N)}$ across the phase transition. The ‘classical’ (versus quantum von Neumann) Rényi-Wehrl entropy is then defined as:

$$W_{N,\nu}(\xi) = \frac{1}{1-\nu} \ln(M_{N,\nu}(\xi)), \quad (14)$$

for $\nu \neq 1$. For $\nu = 1$ we have the usual Wehrl entropy

$$W_N(\xi) = - \int_{\mathbb{R}^4} \Psi_\xi^{(N)}(z_1, z_2) \ln(\Psi_\xi^{(N)}(z_1, z_2)) d\mu(z_1, z_2). \quad (15)$$

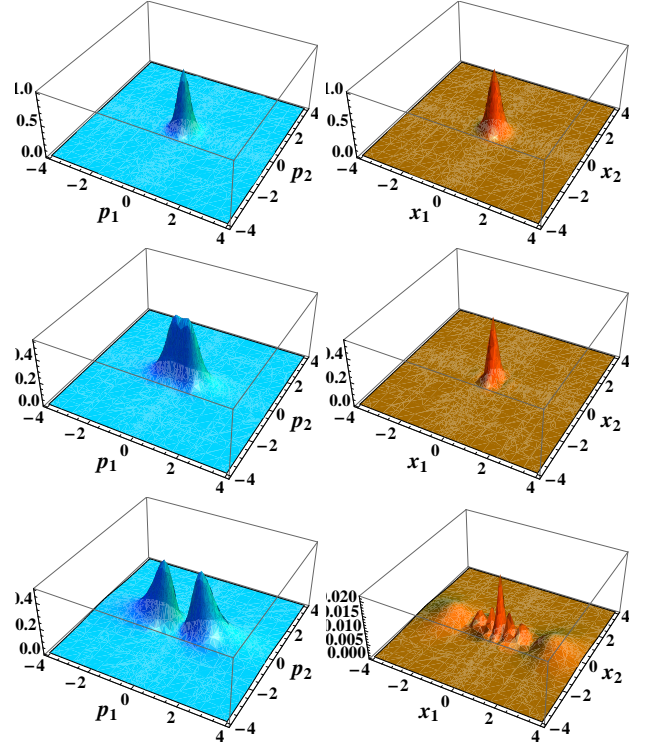


FIG. 1: (Color online) Exact Husimi distribution $\Psi_\xi^{(N)}(z_1, z_2)$ as a function of $z_{1,2} = x_{1,2} + ip_{1,2}$ in ‘momentum space’ ($z_{1,2}$ imaginary; left panel) and ‘position space’ ($z_{1,2}$ real; right panel) for different values of ξ (from top to bottom: $\xi = 0$, $\xi = 0.3$ and $\xi = 0.98$) for $N = 8$. Dimensionless units.

C. Numerical Results

We have solved the vibron-model numerically, calculating the coefficients $c_{nm}^{(N)}(\xi)$ in (10) by numerical diagonalization of (2).

Let us denote by $x_{1,2} = \text{Re}(z_{1,2})$ ‘position’ coordinates and by $p_{1,2} = \text{Im}(z_{1,2})$ ‘momentum’ coordinates. In Figure 1 we represent the Husimi distribution in position ($p_{1,2} = 0$) and momentum ($x_{1,2} = 0$) cross sections. We observe that $\Psi_\xi^{(N)}(ip_1, ip_2)$ splits into two packets for $\xi \geq \xi_c = 0.2$ whereas $\Psi_\xi^{(N)}(x_1, x_2)$ acquires a modulation above the critical point ξ_c . We shall see below how this ‘delocalization’ of the ground state is captured by moments and Wehrl entropy of the Husimi distribution. We have calculated the second moment $M_{N,2}$ (also called ‘inverse participation ratio’ P_N) and the Wehrl entropy W_N as a function of ξ . The computed results are given in Fig. 2 (together with the variational results of Section III), where we present $P_N(\xi)$ and $W_N(\xi)$ for $N = 4, 8, 16$. Notice that the inverse participation ratio (top panel) is greater in the linear phase $\xi < 0.2$ than in the bent phase $\xi > 0.2$, thus capturing the delocalization of the Husimi distribution of the ground state across the critical point $\xi_c = 0.2$ as depicted in Figure 1. Note also that P_N decreases with N , reaching the lim-

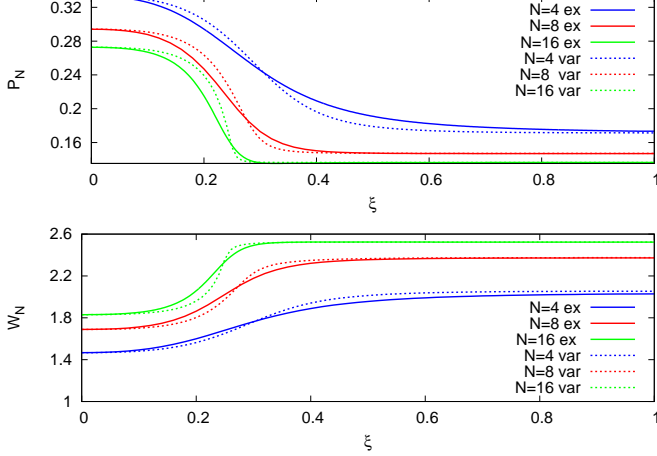


FIG. 2: (Color online) Exact-numerical (solid) against variational-cat (dotted) inverse participation ratio $P_N(\xi)$ and Wehrl's entropy $W_N(\xi)$ for $N = 4, 8$ and $N = 16$ (P_N decreases and W_N increases with N) as a function of ξ . Dimensionless units.

iting values of Eq. (27) for $\nu = 2$. The Wehrl entropy (bottom panel) shows an entropy excess of $0.69 \simeq \ln(2)$ [see later on Eq. (28)], thus capturing the splitting of the Husimi distribution into two non-overlapping packets in the second (bent) phase. The change of $P_N(\xi)$ and $W_N(\xi)$ across ξ_c is more sudden as N increases. Figure 2 also shows a good agreement between the numerical results and a variational approximation given in terms of ‘parity-symmetry-adapted coherent states’ introduced in [23] and discussed in the next section, where we shall provide analytical explicit expressions for moments and Wehrl's entropy as a function of N, ν and ξ and we shall discuss the thermodynamic limit $N \rightarrow \infty$.

III. VARIATIONAL APPROXIMATION AND THE THERMODYNAMIC LIMIT

Now we present analytical expressions for the Husimi distribution, moments and entropies using trial states expressed in terms of ‘parity-symmetry-adapted’ CSs (Schrödinger catlike or ‘cat’ states for short) introduced by us in this context in [23], which turn out to be a good approximation to the exact (numerical) solution of the ground state of the vibron model. In particular, it has been proved in [23] that this parity-symmetry-adapted CS captures the correct behavior for ground-state properties sensitive to the parity symmetry of the Hamiltonian like vibration-rotation entanglement and delocalization measures.

A. Parity-symmetry-adapted CSs and their Husimi distribution

There are strong evidences that the exact ground state (10) can be *itself* nicely approximated by a $SU(3)$ CS of the type (4), when properly adapted to the parity symmetry (see [23] for more details). In fact, using the notation (4), the particular (two-parameter) choice of ‘boson-condensate’ denoted by

$$|N; r, \theta\rangle \equiv |z_1 = -\frac{r}{\sqrt{2}}e^{-i\theta}, z_2 = \frac{r}{\sqrt{2}}e^{i\theta}\rangle \quad (16)$$

[with r, θ , variational parameters representing polar coordinates] has been considered in Ref. [5] as a variational trial state to reproduce the ground state energy in the thermodynamic limit $N \rightarrow \infty$. Note that here z_1 and z_2 are not arbitrary complex numbers, but constrained to $z_1 = -\bar{z}_2$. As a comment, intrinsic excitations can also be constructed in this way, thus defining ‘multi-species CSs’ (see e.g. [24, 25]).

The variational parameter r is fixed by minimizing the ground state energy functional ‘per particle’ (see [5] for more details):

$$\begin{aligned} \mathcal{E}_\xi(r) &= \frac{\langle \hat{H} \rangle}{N} = (1 - \xi) \frac{\langle \hat{n} \rangle}{N} + \xi \frac{N(N+1) - \langle \hat{W}^2 \rangle}{N(N-1)} \\ &= (1 - \xi) \frac{r^2}{1 + r^2} + \xi \left(\frac{1 - r^2}{1 + r^2} \right)^2 \end{aligned} \quad (17)$$

where we have used here $\langle \cdot \rangle$ as a shorthand for expectation values in $|N; r, \theta\rangle$. Note that \mathcal{E}_ξ does not depend on θ because of the intrinsic rotational symmetry, so that we shall restrict ourselves to $\theta = 0$ and simply write from now on $|N; r\rangle \equiv |N; r, \theta = 0\rangle$. From $\partial \mathcal{E}_\xi(r)/\partial r = 0$ one gets the ‘equilibrium radius’ r_e and the ground state energy \mathcal{E}_ξ as a function of the control parameter ξ (see [5] for more details):

$$\begin{aligned} r_e(\xi) &= \begin{cases} 0, & \xi \leq \xi_c = 1/5 \\ \sqrt{\frac{5\xi-1}{3\xi+1}}, & \xi > \xi_c = 1/5 \end{cases} \\ \mathcal{E}_\xi(r_e(\xi)) &= \begin{cases} \xi, & \xi \leq \xi_c = 1/5 \\ \frac{-9\xi^2+10\xi-1}{16\xi}, & \xi > \xi_c = 1/5. \end{cases} \end{aligned} \quad (18)$$

Then one finds that $d^2\mathcal{E}_\xi(r_e(\xi))/d\xi^2$ is discontinuous at $\xi_c = 1/5$ and the phase transition is said to be of second order.

Although the CS $|N; r_e(\xi)\rangle$ properly describes the mean energy in the thermodynamic limit $N \rightarrow \infty$ (see [5] for more details), it has been recently noticed by us in [23] that it does not capture the correct behavior for other ground state properties sensitive to the parity symmetry Π of the Hamiltonian like, for instance, vibration-rotation entanglement. Here we shall see that the Husimi distribution $\Phi_\xi^{(N)}(z_1, z_2) \equiv |\langle z_1, z_2 | \phi_\xi^{(N)} \rangle|^2$ of $|\phi_\xi^{(N)}\rangle = |N; r_e(\xi)\rangle$ neither captures the delocalization of the ground state across the phase transition displayed in Figure 1 and

quantified by the Wehrl entropy in Figure 2, since it does not have a definite parity like the exact ground state (10) does. Indeed, the explicit expression of the Husimi distribution of $|\phi_\xi^{(N)}\rangle = |N; r_e(\xi)\rangle$ can be calculated, as a function of (z_1, z_2) , through the CS overlap (7) as:

$$\begin{aligned}\Phi_\xi^{(N)}(z_1, z_2) &= |\langle z_1, z_2 | \phi_\xi^{(N)} \rangle|^2 = |\langle z_1, z_2 | z'_1, z'_2 \rangle|^2 \\ &= \frac{|1 - \bar{z}_1 \frac{r_e(\xi)}{\sqrt{2}} + \bar{z}_2 \frac{r_e(\xi)}{\sqrt{2}}|^{2N}}{(1 + |z_1|^2 + |z_2|^2)^N (1 + r_e^2(\xi))^N}\end{aligned}\quad (19)$$

where we have substituted $z'_1 = -r_e(\xi)/\sqrt{2}$, $z'_2 = r_e(\xi)/\sqrt{2}$, as in Eq. (16) for $\theta = 0$ and $r = r_e(\xi)$. This distribution $\Phi_\xi^{(N)}(z_1, z_2)$ has a single maximum at $(z_1^{(0)}, z_2^{(0)}) = (-r_e(\xi)/\sqrt{2}, r_e(\xi)/\sqrt{2})$ and therefore does not display the two-packets structure of the exact distribution $\Psi_\xi^{(N)}(z_1, z_2)$ above ξ_c as depicted in Figure 1. We shall also see later in Section IIIB that $\Phi_\xi^{(N)}(z_1, z_2)$ has constant Wehrl entropy, $W_N(\xi) = N(3 + 2N)/((N+1)(N+2))$, and therefore it does not capture the QPT at $\xi = 0.2$, where the exact Wehrl entropy undergoes a sudden increase, as displayed in Figure 2.

The problem is that the variational CS $|\phi_\xi^{(N)}\rangle = |N; r_e(\xi)\rangle$ does not have a definite parity, unlike the exact ground state $|\psi_\xi^{(N)}\rangle$, which has even-parity. A far better variational description of the ground state is given in terms of the even-parity projected CS (see [23] for more details):

$$|N; r, +\rangle \equiv \frac{(1 + \hat{\Pi})|N; r\rangle}{\mathcal{N}_+(r)} = \frac{|N; r\rangle + |N; -r\rangle}{\mathcal{N}_+(r)}, \quad (20)$$

where $\mathcal{N}_+(r) = \sqrt{2}(1 + \langle N; -r | N; r \rangle)^{1/2}$ is a normalization constant, with (remember the CS overlap (7))

$$\langle N; -r | N; r \rangle = ((1 - r^2)/(1 + r^2))^N. \quad (21)$$

Since $\langle N; -r | N; r \rangle \rightarrow 0$ when $N \rightarrow \infty$, the even-parity state (20) is a superposition of two weakly-overlapping (distinguishable) quasi-classical (coherent) wave packets, which justifies the term ‘Schrödinger catlike’ for these states. Parity-symmetry-adapted CSs (of other kind) have also been proposed in [26, 27], and used by us in [17, 20, 21], to study the Dicke model QPT. In particular, in [21] we analyze the Husimi distribution (exact and variational) of the ground state in the Dicke model, which shares some features with the present vibron model.

The variational parameter r in (20) is again computed by minimizing the ground state energy functional ‘per particle’ $\mathcal{E}_{\xi,+}^{(N)}(r) = \langle \hat{H} \rangle_+/N$ as in (17), but now for the symmetric configuration (20), given in terms of the new mean values:

$$\begin{aligned}\frac{\langle \hat{n} \rangle_+}{N} &= \frac{r^2((1 + r^2)^{N-1} - (1 - r^2)^{N-1})}{(1 + r^2)^N + (1 - r^2)^N}, \\ \frac{\langle \hat{W}^2 \rangle_+}{N} &= 2 \frac{(1 + r^2)^N + (1 - r^2)^{N-2}(1 + 2Nr^2 + r^4)}{(1 + r^2)^N + (1 - r^2)^N}.\end{aligned}\quad (22)$$

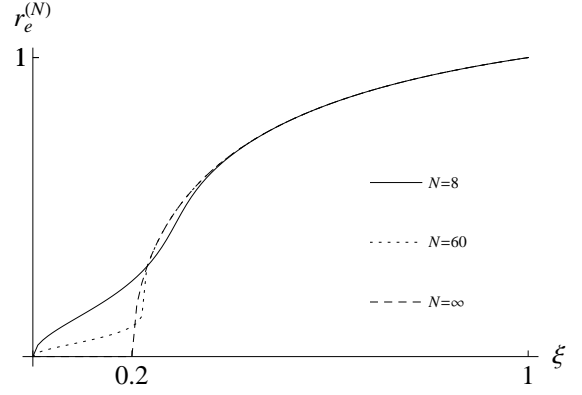


FIG. 3: Equilibrium radius $r_e^{(N)}(\xi)$ for $N = 8, 60, \infty$, where we are identifying $r_e^{(\infty)}(\xi) = r_e(\xi)$. Dimensionless units.

Unlike $\mathcal{E}_\xi(r)$, the new energy functional $\mathcal{E}_{\xi,+}^{(N)}(r)$ depends on N . From $\partial \mathcal{E}_{\xi,+}^{(N)}(r)/\partial r = 0$ we can obtain the new equilibrium radius $r_e^{(N)}(\xi)$. We do not have an explicit analytic expression of $r_e^{(N)}(\xi)$ (as we did for $r_e(\xi)$ in (18)) for arbitrary N and ξ , but one can always compute it numerically. Figure 3 compares $r_e(\xi)$ in (18) with $r_e^{(N)}(\xi)$ for $N = 8$ and $N = 60$. We can infer that, in the thermodynamic limit, $r_e^{(\infty)}(\xi) = r_e(\xi)$. This is a curious fact.

The Husimi distribution of the (even) cat state $|\phi_{\xi,+}^{(N)}\rangle \equiv |N; r_e^{(N)}(\xi), +\rangle$ in (20) is then

$$\begin{aligned}\Phi_{\xi,+}^{(N)}(z_1, z_2) &= |\langle z_1, z_2 | \phi_{\xi,+}^{(N)} \rangle|^2 \\ &= \frac{|\langle z_1, z_2 | N; r \rangle + \langle z_1, z_2 | N; -r \rangle|^2}{\mathcal{N}_+^2(r)},\end{aligned}\quad (23)$$

with

$$\langle z_1, z_2 | N; \pm r \rangle = \frac{(1 \mp \frac{r}{\sqrt{2}}\bar{z}_1 \pm \frac{r}{\sqrt{2}}\bar{z}_2)^N}{(1 + |z_1|^2 + |z_2|^2)^{N/2}(1 + r^2)^{N/2}}, \quad (24)$$

where we must understand now $r = r_e^{(N)}(\xi)$. Since $|\langle z_1, z_2 | N; \pm r \rangle|$ is maximum at $(z_{1,\pm}^{(0)}, z_{2,\pm}^{(0)}) = (\mp \frac{r}{\sqrt{2}}, \pm \frac{r}{\sqrt{2}})$, the variational Husimi distribution (23) captures the exact two-packets structure displayed in Figure 1, although rotated $\pi/4$. Moments and Wehrl’s entropy are insensitive to this global rotation, so that we keep this variational state for which explicit expressions and calculations turn out to be simpler.

B. Moments and Wehrl-Lieb conjecture

Explicit analytic expressions for the ν -th moment $M_{N,\nu}^+$ of the variational-cat Husimi distribution (23) are easily obtained for the rigidly linear phase $\xi = 0$ ($r =$

$r_e^{(N)}(0) = 0$) giving:

$$\begin{aligned} M_{N,\nu}^+(0) &= \int_{\mathbb{R}^4} (\Phi_{0,+}^{(N)}(z_1, z_2))^\nu d\mu(z_1, z_2) \\ &= \frac{(N+1)(N+2)}{(1+\nu N)(2+\nu N)}, \end{aligned} \quad (25)$$

which are in complete agreement with exact-numerical calculations, as displayed in Figure 2 for the particular case of $\nu = 2$. The same happens to the Wehrl entropy for $\xi = 0$, which can be obtained as:

$$W_N^+(0) = \lim_{\nu \rightarrow 1} \frac{1}{1-\nu} \ln M_{N,\nu}^+(0) = \frac{N(3+2N)}{(N+1)(N+2)}. \quad (26)$$

For other values of ξ , integrals can always be numerically done (see e.g. Figure 2 for $M_{N,2}(\xi)$ and $W_N(\xi)$ as a function of ξ for $N = 4, 8, 16$). In the rigidly bent phase $\xi = 1$, we have been able to obtain the asymptotic behavior for $N \rightarrow \infty$, in particular:

$$M_{N,\nu}^+(\xi) \xrightarrow{N \rightarrow \infty} \begin{cases} \nu^{-2}, & \text{if } \xi = 0 \\ 2^{1-\nu} \nu^{-2}, & \text{if } \xi = 1, \end{cases} \quad (27)$$

and

$$W_N^+(\xi) \xrightarrow{N \rightarrow \infty} \begin{cases} 2, & \text{if } \xi = 0 \\ 2 + \ln(2), & \text{if } \xi = 1. \end{cases} \quad (28)$$

In fact, expressions (27) and (28) also give a good approximation for $N \gg 1$ in the ‘floppy’ region $0 < \xi < 1$ since changes in moments and Wehrl entropy are sharper and sharper as N increases, both being approximately constant in each phase as inferred in Figure 2.

At this point, one could ask himself/herself to what extent are the results for the parity-symmetry-adapted CS (20) better or different from the ordinary CS ansatz (16). We must say that Wehrl entropy for the Husimi distribution $\Phi_\xi^{(N)}$ of the (ordinary) CS (16) is *constant*, $W_N(\xi) = N(3+2N)/((N+1)(N+2))$, as a function of the control parameter ξ (through the dependence of $r = r_e(\xi)$) and, therefore, it does not capture the delocalization of the ground state across the phase transition displayed in Figure 1 and quantified by the IPR and Wehrl entropy in Figure 2. On the contrary, the Husimi distribution $\Phi_{\xi,+}^{(N)}$ in Eq. (23) nicely captures this delocalization, exhibiting an entropy excess of $\ln(2)$ from linear to bent phases, in agreement with exact numerical results.

We should also point out that the behavior displayed in (27) and (28) has also been found by us in the Dicke model of matter-field interactions in the thermodynamic limit $N = 2j \rightarrow \infty$ (the number of atoms), which also exhibits a QPT from normal to superradiant (see [21]).

To finish this section, we would like to comment on the still unproved Lieb’s conjecture. It was conjectured by Wehrl [28] and proved by Lieb [29] that any Glauber (harmonic oscillator) coherent state $|\alpha\rangle$ has a minimum Wehrl entropy of 1. In the same paper by Lieb [29], it

was also conjectured that the extension of Wehrl’s definition of entropy for spin- j CSs (6) will yield a minimum entropy of $2j/(2j+1)$. Here we propose that the extension (15) of Lieb’s definition of entropy will yield a minimum entropy of $N(3+2N)/((N+1)(N+2))$ for $SU(3)$ projective CSs (4). We have seen that the ground state of the vibron model in the rigidly linear phase ($\xi = 0$) is itself a $SU(3)$ CS and its Wehrl entropy reaches this minimum. The same value is attained for the Wehrl entropy of any other $SU(3)$ CS like (4). In the rigidly bent phase ($\xi = 1$), the ground state is not a $SU(3)$ CS anymore, but has a “cat-like” structure (linear combination of CSs) giving a Wehrl entropy excess of $\ln(2)$.

C. Zeros of the variational Husimi distribution

It is well known that the Husimi density is determined by its zeros through the Weierstrass-Hadamard factorization. It has also been observed that the distribution of zeros differs for classically regular or chaotic systems and can be considered as a quantum indicator of classical chaos (see e.g. [9, 11, 12]). Moreover, recently we have presented a characterization of the Dicke model QPT by means of the zeros of the Husimi distribution in the variational approach [21].

Here we shall explore the distribution of zeros of the Husimi density as a fingerprint of QPT in the vibron model. From (23) we obtain

$$\Phi_{\xi,+}^{(N)}(z_1, z_2) = 0 \Rightarrow z_2 - z_1 = \frac{i\sqrt{2}}{r_e^{(N)}(\xi)} \tan\left(\frac{(2l+1)\pi}{2N}\right) \quad (29)$$

with $l = -[N/2], \dots, [N/2] - 1$ and $[N/2] = \text{Floor}(N/2)$. If we separate real and imaginary parts as $z_{1,2} = x_{1,2} + ip_{1,2}$, the last condition can be cast as

$$x_1 = x_2, \quad (30)$$

$$p_2 = p_1 + \frac{\sqrt{2}}{r_e^{(N)}(\xi)} \tan\left(\frac{(2l+1)\pi}{2N}\right). \quad (31)$$

For $r_e^{(N)}(\xi) = 0$ the Husimi distribution $\Phi_{\xi,+}^{(N)}(z_1, z_2)$ has no zeros. For finite N , the value $r_e^{(N)}(\xi) = 0$ is only attained in the rigidly linear phase $\xi = 0$ (see Figure 3). In the thermodynamic limit $N \rightarrow \infty$ we have that $r_e^{(\infty)}(\xi) = r_e(\xi) = 0, \forall \xi < \xi_c = 0.2$ (See Figure 3 and expression (18)) so that $\Phi_{\xi,+}^{(\infty)}(z_1, z_2)$ has no zeros in the linear phase. For $r_e^{(N)}(\xi) \neq 0$ the zeros are localized along straight lines (“dark fringes”) in the $x_1 x_2$ (position) and $p_1 p_2$ (momentum) planes. In the momentum plane, the density of zeros grows with N and ξ (viz, with $r_e^{(N)}(\xi)$, since it is an increasing function of ξ). In the thermodynamic limit $N \rightarrow \infty$, there is a sudden growth of zeros for $\xi > \xi_c = 0.2$ which accumulate in a vicinity of $p_2 = p_1$ in the momentum plane $p_1 p_2$. A similar behavior is also shared by the Dicke model (see [21]).

IV. CONCLUSIONS

We have found that moments and Wehrl entropies of the Husimi distribution provide sharp indicators of a quantum phase transition in the vibron model. They detect a delocalization of the Husimi distribution across the critical point ξ_c and we have employed them to quantify the phase-space spreading of the ground state.

Calculations have been done numerically and through a variational approximation. We have represented the Husimi distribution which exhibits a different shape in each phase. We have calculated the inverse participation ratio and the Wehrl entropy, which prove to be good indicators of the QPT. The variational approach, in terms of parity-symmetry-adapted coherent (cat) states, complements and enriches the analysis providing explicit analytical expressions for the moments and Wehrl entropies which remarkably coincide with the numerical results, especially in the rigidly linear and bent phases (outside the floppy region $\xi \approx \xi_c$) and in the thermodynamic limit.

In the rigidly linear phase, Wehrl's entropy attains its minimum $\frac{N(3+2N)}{(N+1)(N+2)}$, according to a generalized Wehrl-Lieb conjecture, thus indicating that the ground state for $\xi = 0$ is a $SU(3)$ projective CS. In the bent phase, Wehrl's entropy undergoes an entropy excess (or "subentropy" [30]) of $\ln(2)$. This fact implies that the Husimi distribution splits up into two identical subpackets with negligible overlap in passing from linear to bent phase; in general, for s identical subpackets with negligible overlap, one would expect an entropy excess of $\ln(s)$. This delocalization of the exact Husimi distribution in the bent phase is not captured by the variational approximation in terms of the ordinary $SU(3)$ CS (16), which gives a constant value of IPR P_N and Wehrl entropy W_N

across the phase transition. On the contrary, the parity-symmetry-adapted CS of eq. (20) nicely reproduces the exact ground state behavior, as seen in figure 2.

The QPT fingerprints in the vibron model have also been tracked by exploring the distribution of zeros of the Husimi density within the analytical variational approximation. We have found that there is a sudden growth of zeros above the critical point ξ_c , specially in the thermodynamic limit. Zeros of the variational Husimi (cat) distribution exhibit a richer structure in momentum than in position space. This behavior is also shared by the Dicke model [21]. This subject deserves further attention and will be studied in future works.

The different structure of zeros of the Husimi distribution for classically regular or chaotic systems has also been considered in the literature as a quantum indicator of classical chaos (see e.g. [9, 11, 12]). For example, in [12] it is shown that, in integrable regions, the zeros lie on one-dimensional curves, while in chaotic regions the distribution is bi-dimensional and the zeros fill the phase-space. We have restricted ourselves to the phase-space analysis of the ground state in the vibron-model. The vibron-model is a regular (non chaotic) system so we can assert that the sudden growth of zeros above the critical point ξ_c denotes a QPT but it is not a symptom of chaos.

Acknowledgments

This work was supported by the Projects: FIS2011-24149 and FIS2011-29813-C02-01 (Spanish MICINN), FQM-165/0207 and FQM219 (Junta de Andalucía) and 20F12.41 (CEI BioTic UGR).

-
- [1] S. Sachdev, *Quantum Phase Transitions*, Cambridge University Press (2000).
 - [2] F. Iachello, *Algebraic theory of Molecules*, Oxford University Press (1995).
 - [3] F. Iachello, J. Chem. Phys. **78**, 581 (1981).
 - [4] F. Iachello, S. Oss, J. Chem. Phys. **104**, 6956 (1996).
 - [5] F. Pérez-Bernal, F. Iachello, Phys. Rev. A **77**, 032115 (2008).
 - [6] R. H. Dicke, Phys. Rev. **93**, 99 (1954).
 - [7] C. C. Gerry and P. L. Knight, *Introductory Quantum Optics*, Cambridge University Press (2005).
 - [8] C. Aulbach, A. Wobst, G.-L. Ingold, P. Hanggi and I. Varga, New J. of Physics **6**, 70 (2004).
 - [9] P. A. Dando and T. S. Monteiro, J. Phys. B. **27**, 2681, (1994).
 - [10] D. Weinmann, S. Kohler, G.-L. Ingold and P. Hänggi, Ann. Phys. (Lpz) **8** SI277 (1999).
 - [11] H. J. Korsch, C. Müller and H. Wiescher, J. Phys. A **30**, L677 (1997).
 - [12] P. Leboeuf and A. Voros, J. Phys. A **23**, 1765 (1990).
 - [13] P. A. Dando, and T. S. Monteiro, J. Phys. B **27**, 2681 (1994).
 - [14] F. Mintert and K. Życzkowski, Phys. Rev. A **69**, 022317 (2004).
 - [15] E. Romera and Á. Nagy, Phys. Lett. A **375** 3066 (2011).
 - [16] E. Romera, K. Sen and Á. Nagy, J. Stat. Mech. (2011) P09016.
 - [17] E. Romera, M. Calixto and Á. Nagy, Europhys. Lett. **97**, 20011 (2012).
 - [18] Á. Nagy and E. Romera, Physica A **391**, 3650 (2012).
 - [19] E. Romera, R. del Real, M. Calixto, S. Nagy and A. Nagy, *Rényi entropy of the vibron model*, submitted (2012).
 - [20] M. Calixto, Á. Nagy, I. Paraleda and E. Romera, Phys. Rev. A **85**, 053813 (2012).
 - [21] E. Romera, R. del Real and M. Calixto, Phys. Rev. A **85**, 053831 (2012).
 - [22] A. Perelomov, *Generalized Coherent States and Their Applications*, Springer-Verlag (1986).
 - [23] M. Calixto, E. Romera and R. del Real, J. Phys. A **45**, 365301 (2012).
 - [24] S. Kuyucak and M. K. Roberts, Phys. Rev. A **57**, 3381 (1998).
 - [25] M.A. Caprio, J. Phys. (Math. Gen.) **A38**, 6385 (2005)

- [26] O. Castaños, E. Nahmad-Achar, R. López-Peña and J. G. Hirsch, Phys. Rev. A **83**, 051601 (2011).
- [27] O. Castaños, E. Nahmad-Achar, R. López-Peña, and J. G. Hirsch, Phys. Rev. A, **84** 013819 (2011).
- [28] A. Wehrl, Rep. Math. Phys. **16**, 353 (1979)
- [29] E.H. Lieb, Commun. Math. Phys. **62**, 35 (1978)
- [30] R. Jozsa, D. Robb and W.K. Wootters, Phys. Rev. A **49**, 668 (1994).